

# Femto-Macro Cellular Interference Control with Subband Scheduling and Interference Cancellation

Sundeep Rangan, *Member, IEEE*

**Abstract**—A significant technical challenge in deploying femtocells is controlling the interference from the underlay of femtos onto the overlay of macros. This paper presents a novel interference control method where the macrocell bandwidth is partitioned into subbands, and the short-range femtocell links adaptively allocate their power across the subbands based on a load-spillage power control method. The scheme can improve rate distribution in the macro network while also providing opportunities for short-range communication as well. Moreover, the proposed scheme requires minimal interference coordination communication between the femtos and macros, which is one of the main challenges in femtocell systems. Also, simulations show certain advantages over simpler orthogonalization schemes or power control schemes without subband partitioning. Further modest gains may also be possible with interference cancellation.

**Index Terms**—Femtocells, interference coordination, cellular systems, wireless communications, interference cancellation, fractional frequency reuse.

## I. INTRODUCTION

Femtocells are small wireless access points that are typically installed in a subscriber's premises, but operate in a cellular provider's licensed spectrum. Since femtocells can be manufactured at a very low cost, require minimal network maintenance by the operator and can leverage the subscriber's backhaul, femtocells offer the possibility of expanding cellular capacity at a fraction of the cost of traditional macrocellular deployments. With the surge in demand for wireless data services, femtocells have thus attracted considerable recent attention, both in cellular standards bodies such as the 3GPP (Third Generation Partnership Program) [1], [2], [3] and academic research [4], [5].

However, one of the key technical challenges in deploying femtocells is the interference between the underlay of small femtocells and the overlay of comparatively large macrocells [4], [6], [7]. This *cross-tier* interference problem differs from interference problems in traditional macrocellular networks in several important aspects: First, due to *restricted association*, mobile terminals (called user equipment or UEs in 3GPP terminology) may not be able to connect to a given femtocell even when it provides the closest serving base station. Such restrictions can result in strong interference both from the macro UE transmitter onto the femto uplink and from the femto downlink onto the macro UE receiver. Second, since femtocells are generally not connected directly into the operator's core network, and instead go through the

subscriber's private ISP, backhaul signaling for interference coordination is often more limited. In addition, over-the-air signaling may also be difficult due to the power disparities between the femtos and macros, and the large number of femtos per macro. Finally, femtos are usually deployed in an *ad hoc* manner as opposed to carefully planned deployments in macrocellular networks. Such deployments further degrade interference and also require that any interference coordination be self-configuring and adaptive.

To address these problems, this paper proposes a novel method for macro-femto interference control based on subband scheduling, power control and, if available, interference cancellation. In the proposed method, both the uplink (UL) and downlink (DL) bands of the macrocell overlay network are first partitioned into *subbands*. Using standard fractional frequency reuse (FFR) methods [8], [9], [10], [11], the macro transmit power is varied across the subbands to create different reuse patterns and interference conditions in each subband. It is well-known that this subband partitioning can improve the rate distribution in the macro network.

Following the observations of [12], the basic thesis of this paper is that subband partitioning can also create improved opportunities for femtocell communication as well. Specifically, we argue that, when the macrocell network employs subband partitioning, most femto links will be able to transmit in one or more subbands with minimal interference into the macro network. Moreover, using a *load-spillage* power control method similar to [13], we provide a practical method by which femto transmitters can identify the interference effect in each subband and optimize their power distribution across the subbands appropriately.

There are several appealing features of the proposed interference control method:

- *Minimal cross-tier communication*: The proposed method requires no explicit cross-tier communication between the femto and macrocells. As discussed above, femto-macro coordination communication is logistically difficult. The proposed load-spillage method avoids such communication and simply requires that the macro base stations measure the total noise rise due to the femtos and broadcast a *load* factor. The femtocell transmitters read the load factor and adjust their transmit power according to a simple rule.
- *Frequency reuse*: As described in [12], the subband partitioning enables the spectrum to be reused efficiently between the femto and macrocells. Our simulations reveal that, when combined with optimal power allocation across the subbands, the subband partitioning can result

S. Rangan (email: srangan@poly.edu) is with Polytechnic Institute of New York University, Brooklyn, NY.

in significant additional throughput in the same spectrum as the macro. This throughput can be higher than orthogonalization between the femto and macro layers, and – at least in the UL – higher than the throughput with simple reuse 1 without subband scheduling.

- *Improved throughput with interference cancelation:* Finally, we show in simulations that modest throughput gains may also be possible when the femto receivers are capable of interference cancelation via joint detection of the desired signal and interfering macro signal.

#### A. Previous Work

A general introduction on femtocells, including descriptions of the femto-macro interference problem, can be found in the recent text [14], as well as several general papers [4], [5], [7], [6]. To address the femto-macro interference problem, a number of works have considered power control and interference mitigation techniques. In addition to the works above, the paper [15], for example, studies adaptive attenuation and power control methods for UMTS femtos, while [16], [17] study more sophisticated power control methods based on distributed utility maximization. These power control methods have the benefit that they can be largely implemented in existing cellular systems, and based on simulations such as the Femto Forum study [18], appear to work well in a range of circumstances. In addition, power control admits precise analyses. For example, the works [19], [20], [21], [22] provide analytic expressions for the outage capacity under power control with various cell selection methods.

The contribution of this paper is to combine these femtocell power control methods with two other concepts: subband partitioning and interference cancelation.

Subband partitioning, and the related concept of fractional frequency reuse (FFR), are well-known in the cellular industry. Some early descriptions can be found in [8], [9] with further analyses for distributed algorithms in [10], [11]. FFR has attracted considerable recent attention since it is particularly easy to implement in OFDMA systems such as in 3GPP's long-term evolution (LTE) standard [23].

However, the application of FFR to the femto-macro interference problem considered here requires some modifications. FFR methods such as [8], [9] employ a static power allocation across the subbands. Static allocations may work well in the macrocellular network where the interference conditions between cell sites are stable. However, short range femto links can have arbitrary and changing locations relative to the macro and thus need adaptive schemes. Several adaptive FFR methods have also been proposed such as [10], [11], but would require coordination between the femto and macros in the context of the problem here. As discussed above, this coordination can be logistically difficult. The method proposed here requires no explicit coordination other than the broadcast of the load factors from the macro receivers. We will see (see Theorem 1) that, when the interference at the femtos is dominated by the macro transmitters, the proposed scheme remains optimal.

Our proposed method also has benefits the femto-macro FFR method in [12]. That work uses the same partitioning

discussed in Section II, but with the femto assigned to a single subband based on the DL SINR. The method proposed here permits the femto UE or BS to transmit on all subbands *simultaneously*. Also, the DL SINR metric used in [12] is indirect measurement that is only statistically correlated to the interference effect of a femto's transmission. This work uses a load-spillage mechanism of [13] to determine the precise interference effect in each subband and allocate the power across the subbands appropriately.

The second main novel component of this paper is interference cancelation (IC) via joint detection of the desired femto signal and interfering macro signal. The theoretical benefits of interference cancelation and joint detection are well-known [24], [25]. Also, due to improved computational resources, successive IC (SIC) has begun to be implemented in commercial cellular systems for both macrocells [26], [27] and femtocells [15]. However, for cellular systems, SIC has been generally used in the UL, where power control can be used to shape the receive powers of multiple mobiles with a favorable profile for SIC. What is new here is that we will show that when subband partitioning is performed in the macrolayer, interference conditions will naturally arise such that IC may be used by the short-range links to cancel the interference from the macro. Unfortunately, we only observe gains with joint detection and not with SIC alone.

It should be pointed out that a limitation in this work is that cell selection between femtos and macros is fixed. In reality, femto-macro cell selection is itself an important problem and typically depends on loading, mobility and whether the femtos employ open or closed access. The reader is referred to [28], [29], [30] for a discussion of these issues.

## II. MACROCELL SUBBAND PARTITIONING

The proposed macro-femto interference control method assumes subband partitioning of the macro overlay network similar to that of Oh *et. al.* in [12]. In subband partitioning, both the UL and DL bands of the macro overlay network are partitioned into *subbands*, which are contiguous non-overlapping frequency intervals. For the macro-femto interference control method, we consider the simple subband partitioning shown in Fig. 1. More general partitions can also be considered.

As shown in the figure, we assume the cell sites in the macrocell network are three way sectorized. Following the 3GPP terminology, we call each sector in the cell site a *cell*. With this sectorization, we partition both the UL and DL bands into four subbands whose center frequencies denoted  $f_0$  to  $f_3$ . With some abuse of notation, we will use  $f_k$  to denote the subband as well as its center frequency.

One of the four subbands,  $f_0$ , is reused in every cell, and will be called the reuse 1 subband. This subband will generally serve mobiles who are close to the cell and is thus shown in the figure in the inner circle of the cell site. Each of the remaining subbands –  $f_1$  to  $f_3$  – is used in only one cell per cell site. These subbands will be called the reuse 3 subbands. The reuse 3 subbands are arranged so that neighboring cells do not use the same subbands, so the interference in these subbands is low. These subbands are used to serve the mobiles

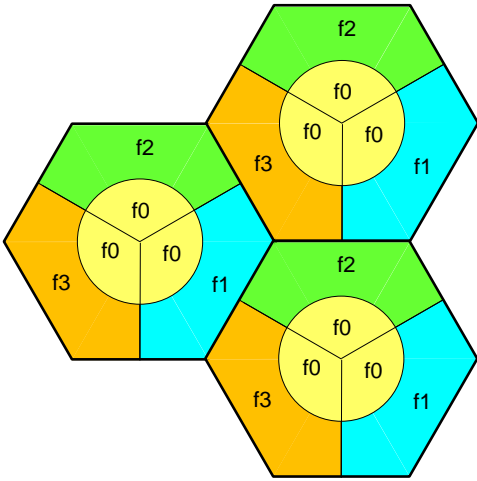


Fig. 1. Subband partitioning of the macrocells. Each cell site occupies one hexagon with the cell site partitioned into three 120 degree sectors called cells. The frequency subband  $f_0$  is used in all cells and serves mobiles close to the cell. The other subbands  $f_1$  to  $f_3$  are used in only cell per cell site and serves mobiles close to the cell edge.

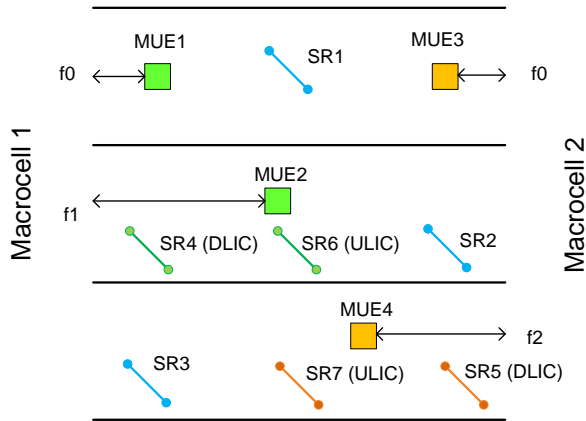


Fig. 2. Typical locations of macro UEs (MUE1–4) in each subband, along with possible locations for short-range links (SR1–7). SR1–3 can operate in either the UL or DL and do not require interference cancellation (IC). SR4 and 5 would operate in the DL with IC of the DL signal from the macrocell base stations. SR6 and 7 operate in the UL with IC of the macro UE transmissions.

at the edge of the cell where the mobile would experience high interference if served in the reuse 1 subband.

The basis of subband partitioning is that in any multiuser wireless system, there is a tradeoff between maximizing the bandwidth (which is obtained by reusing the spectrum in different links), or minimizing interference (which is obtained by orthogonalizing bandwidth in different links). Subband partitioning enables this tradeoff to be optimized differently for mobiles depending on their geometry. Consider, for example, the transmissions of two macrocells in Fig. 2. Macrocell 1 serves two macro UEs, MUE1 and 2, while macrocell 2 serves macro UEs MUE3 and 4. MUE1 and MUE3 are close to their serving cells and thus experience little interference from the other cell. These mobiles can be served in the reuse 1 subband,  $f_0$ , where the full bandwidth of the subband can be reused in both cells. In contrast, MUE2 and 4 are at the cell edge. If served in the same subband, the interference would be high.

For these mobiles, the rate may be higher by serving them on orthogonal bandwidths,  $f_1$  and  $f_2$ , which eliminates the interference from the other cell.

It is well-known that such subband partitioning can often improve the rate distribution in the macrocellular network: usually the edge of cell mobile rate can be increased with a relatively small loss in rate for the good mobiles. However, what is important for this work is the observation of [12] that subband partitioning also creates improved opportunities for short-range transmissions with minimal interference into the macro network. To see this property, consider again Fig. 2 which also shows three possible locations for short range links, labeled SR1 to 3. For now, ignore the short range links SR4–7 which we will discuss in Section IV.

First consider a short-range link, such as SR1, at the macrocell edge (i.e. between the two macrocells). A short range link such as SR1 can operate in the reuse 1 subband,  $f_0$ , in either the UL or DL. For the UL, the short range link is far from either macrocell, so the transmissions should have minimal interference at the macrocell receivers. Also, since the UEs in  $f_0$  are typically close to their cell, they will also be far from SR1. Therefore, transmissions on SR1 in the DL  $f_0$  will also have minimal interference at the macro UEs such as MUE1 and 3.

Now consider the cases, such as SR2 or SR3, when the short range links are close to one of the macrocells. In these cases, the short range links can transmit in one of the subbands  $f_1$  or  $f_2$  not being used by the macrocell that it is close to.

In this way, the subband partitioning provides, wherever the short-range link is located, frequency locations on which it can transmit where the interference will be minimal. This property is the basic observation of [12] and will serve as the basis of the proposed femto-macro interference control method here.

### III. SUBBAND INTERFERENCE POWER CONTROL

In the method in [12], each femtocell transmitter (the femto BS in the DL and femto UE in the UL) is statically assigned to a single subband based on the DL SINR. In the proposed method of this paper, the femtocell transmitter can simultaneously use all subbands, with a power level in each subband based on the precise interference conditions. This method enables a larger fraction of the bandwidth to be used and to select the powers in the subbands based on the actual interference conditions.

To describe the proposed method mathematically, suppose that there are  $K$  total subbands. For example, in the subband partitioning of the previous section, there would be  $K = 4$  subbands in the UL or DL. We will assume there are  $N$  short-range links denoted  $SR_j$ ,  $j = 1, \dots, N$ . We will use the term short-range links, as opposed to femto links, since the method does not require that short-range links using the same technology as the macro. Also, the macrocellular system could be TDD or FDD. In the case of TDD, the short-range links will use the UL and DL time periods aligned with the macro.

We will assume that in subband  $k$ , there are  $M(k)$  macro receivers, which we will denote by  $MRX_{ik}$ ,  $i = 1, \dots, M(k)$ .

In an UL subband, the macro receivers are the macrocell base stations using that subband, and in the DL, the macro receivers are the UEs using that subband.

Now let  $G_{ijk}$  be the path gain from the short-range transmitter  $\text{SRTX}_j$  to the macro receiver  $\text{MRX}_{ik}$  in subband  $k$ . We will let  $p_{jk}$  be the transmit power of  $\text{SRTX}_j$  in subband  $k$ , so that the total interference at  $\text{MRX}_{ik}$  in subband  $k$  from all short-range links is

$$q_{ik} = \sum_{j=1}^N G_{ijk} p_{jk}. \quad (1)$$

To implement the femto-macro interference power control, we will assume that each short range transmitter,  $\text{SRTX}_j$ , can learn the path gains  $G_{ijk}$  to all the macro receivers in all the  $K$  subbands. To perform this estimation in the UL subbands, the macrocell base stations would need to intermittently transmit some reference signal in the UL. Of course, this would require that the regular UL macrocellular transmissions are suspended in some quiet period and thus requires some overhead. Similarly, in the DL, the path losses to the macro UEs could be estimated by having a quiet period in the DL where the macro UEs suspending their regular reception and transmit reference signals that the short-range transmitters can hear. Alternatively, in a TDD system, a short range transmitter could estimate an UL path gain to the base stations from a DL reference such as the pilot signals, and an DL path gain to the macro UEs from the UEs uplink power control signals. These reference signals can also be used in a FDD system, but with some error due to fast fading.

Now let  $\mathbf{p}_j$  be the vector of powers used by  $\text{SRTX}_j$  across the  $K$  subbands,

$$\mathbf{p}_j := [p_{j1} \cdots p_{jK}]^T. \quad (2)$$

The power control problem is for each  $\text{SRTX}_j$  to select the power vector  $\mathbf{p}_j$  to control the interference levels  $q_{ik}$  in (1), while maximizing the throughput. This is a distributed control problem since all the short-range transmitters have some effect on the interference levels.

Under the assumptions we will make below, this power control problem is somewhat trivial and can be solved by a large number of distributed methods. See, for example, the survey [31]. As one possible solution, we present a *load-spillage* method similar to [13]. Each macro receiver  $\text{MRX}_{ik}$  broadcasts a *load factor*, denoted  $s_{ik}$ , on subband  $k$ . The load factor is simply some positive scalar. Each short range transmitter  $\text{SRTX}_j$  then computes a per subband *spillage* given by

$$r_{jk} = \sum_{i=1}^M G_{ijk} s_{jk}. \quad (3)$$

The  $\text{SRTX}_j$  can then select any set of powers  $p_{jk}$  subject to

$$\sum_{k=1}^K r_{jk} p_{jk} \leq \lambda_j, \quad (4)$$

where  $\lambda_j$  is some pre-determined positive scalar which we will call the *power constraint bound*.

The load-spillage rule (4) can be understood qualitatively as follows: The rule (4) permits the short-range links to transmit a high power  $p_{jk}$  precisely when the corresponding spillage  $r_{jk}$  is small. Now, the spillage (3)  $r_{jk}$  is high when there is some macro receiver  $\text{MRX}_{ik}$  that is either close to the short-range transmitter (so that  $G_{ijk}$  is large) or the macro receiver broadcasts a high load factor  $s_{ik}$ . Thus, the spillage rule (4) will cause the short-range transmitters to allocate power away from subbands where there are close by macro receivers or macro receivers indicating high load.

We can, in fact, mathematically show that under certain simplifying assumptions, the load spillage rule can be optimal. Specifically suppose that, associated with each short-range link  $j$ , there is some ‘‘utility’’  $U_j(\mathbf{p}_j)$  of the powers  $\mathbf{p}_j$ . This utility could be, for example, the rate or some function of the rate. The implicit assumption is that the utility does not depend on the power levels in other short-range links. That is, the interference at the short-range receivers is dominated by the interference from the macro transmissions.

Given such a utility function and power constraint (4), a natural strategy for each short-range transmitter  $\text{SRTX}_j$  is to select the power vector  $\mathbf{p}_j$  to maximize the utility:

$$\max_{\mathbf{p}} U_j(\mathbf{p}_j) \quad (5)$$

subject to (4). In the case when  $U_j(\mathbf{p}_j)$  is the total rate across the  $K$  subbands, and the rate is given by the Shannon capacity, this optimization reduces to a standard waterfilling procedure [25].

However, whatever the utility function  $U_j(\mathbf{p}_j)$ , we can show the following result: Say a selection of power vectors  $\mathbf{p} = \{\mathbf{p}_j, j = 1, \dots, N\}$  is *Pareto optimal* if any other selection of power vectors that results in a lower interference  $q_{ik}$  on some subband  $k$  for some macro receiver  $\text{MRX}_{ik}$ , or higher utility  $U_j$  for some short range link  $\text{SR}_j$ , must also result in a higher interference for some other macro receiver or lower utility in some other link.

*Theorem 1:* Suppose that the utility functions  $U_j(\mathbf{p}_j)$  are strictly increasing in each component  $p_{jk}$ . Then,

- If the load factors  $s_{ik}$  and power constraint bounds  $\lambda_j$  are positive and each short-range link  $j$  selects the power vector according to (5), then the resulting power vectors are Pareto optimal.
- If, in addition, the utility functions are concave and twice differentiable and  $G_{ijk} > 0$  for all  $i, j$  and  $k$ , then the converse is true. That is, if  $\mathbf{p}$  is any set of power vectors that is Pareto optimal, then there exists nonnegative  $s_{ik}$  and  $\lambda_j$  such that each  $\mathbf{p}_j$  satisfies (5).

*Proof:* See Appendix A. ■

The consequence of the theorem is that the load factors  $s_{ik}$  and  $\lambda_j$  provide a parametrization of all the Pareto optimal power vectors. Thus, the power vectors obtained for any  $s_{ik}$  and  $\lambda_j$  are guaranteed to be Pareto optimal. Moreover, by appropriately selecting the parameters, any optimal point can be achieved.

However, it is important to recognize some caveats. Most importantly, as mentioned above, the implicit assumption in the utility function is that the power selection in one short

range link does not affect other short-range links. This assumption is valid when the interference at the short range links is dominated by either thermal noise or interference from the macro transmitters. When there is significant interference between short-range links, the problem is significantly more complex. In fact, when  $K > 1$ , the problem is similar to the parallel channel interference power control problem that arises in DSL cross-talk [32]. This problem is generally non-convex and NP-hard. The load spillage method can be extended to provide a suboptimal solution to the problem. For example, following the lines of [33], the short-range receivers could themselves broadcast load factors and have their interference counted in the spillage term (3). This procedure would at best converge to some local maxima.

Also, while the theorem states that, in theory, any Pareto optimal power vector is achievable, it provides no mechanism for selecting the appropriate load factors  $s_{ik}$  or bounds  $\lambda_j$ . In the simulations below, the macro receivers will select the load factors  $s_{ik}$  simply based on measuring the noise rise and adjusting the load factors to keep the noise rise at a given target. However, selection of the bounds  $\lambda_j$  or optimal selection of the load factors  $s_{ik}$  would generally require some femto-macro communication which we are not considering.

There is indeed significant possibilities for more sophisticated interference coordination here. However, we will not consider such methods in this work, as our main objective here is to show that, even simple power control methods that use minimal coordination can provide good performance.

#### IV. INTERFERENCE CANCELATION

The proposed femto-macro interference control method can also be used in conjunction with interference cancelation (IC) [25] for further throughput gains. To see this, suppose that the short-range receiver has the computational ability to perform IC on the macrocellular signals. Now return again Fig. 2 and consider first the short range links SR4 and SR5. SR4, being close to macrocell 1, will receive the DL signal on  $f_1$  strongly. Also, the signal on that subband will typically be at low rate since it is intended for an edge of cell mobile, MUE2. Thus, with a high probability, the receiver on SR4 will be able to jointly decode and cancel the interfering signal from macrocell 1 while receiving the signal from its desired transmitter. Similarly, the receiver SR5 can perform IC with high likelihood on the DL signal from macrocell 2 on  $f_2$ .

Now for the UL, consider short-range links SR 6 and 7. These links are close to the macro UEs, MUE 2 and 3. Since MUE 2 and 3 are far from their serving macrocell, they will likely transmit at a low rate, and thus can be canceled by the nearby short range receivers.

In this way, we see that when the short range link receivers are capable of IC, with high likelihood, the interference cancelation may be able to remove interference in a number of the subbands. Moreover, IC can be performed entirely opportunistically in that the macro does not need to change its scheduler policy at all, or even be aware of the short-range links. The regular operation of the macro under the subband partitioning will naturally open up possibilities where IC can be used.

Parameter	Value
Macro topology	24 hexagonal cell sites with wrap around and 3 cells per site.
Femto layout	Uniformly distributed at density of 10 per macrocell
Number macro UEs	10 per macrocell.
Numer femto UEs	1 per femtocell.
Macro cell radius	500 m
Femto link distance	20 m
Macro antenna pattern	$A(\theta) = -\min \left\{ 12 \left( \frac{\theta}{\theta_{3dB}} \right)^2, A_m \right\}$ , $\theta_{3dB} = 70$ degrees and $A_m = 20$ dB
Femto antenna pattern	Omnni
Lognormal shadowing (macro BS involved)	8.1 dB, 50% inter-site correlation; 100% intra-site correlation
Lognormal shadowing (macro BS not involved)	4 dB, no correlation

TABLE I  
PARAMETERS FOR SIMULATION OF THE FEMTO-MACRO INTERFERENCE  
POWER CONTROL ALGORITHM.

#### V. NUMERICAL SIMULATION

The method was evaluated under a simulation model similar to Femto Forum interference management study in [18] with parameters shown in Table I. The macro network is composed of a 24 hexagonal cell sites arranged in a 4 x 6 grid with wrap around to eliminate edge effects. Each site has three cells with the antenna pattern  $A(\theta)$  given in Table I. The bandwidth is partitioned into reuse 1 and reuse 3 subbands as described in Section II, with a fraction  $p_1 = 0.5$  of the bandwidth allocated to the reuse 1 subband.

Macro UEs are distributed uniformly with an average of 10 macro UEs per macrocell. We assume that the macro UEs connect to the strongest macrocell. In each cell, the fraction  $p_1$  of the macro UEs with the highest SINR are assigned to the reuse 1 subband, and the remaining fraction of  $1 - p_1$  macro UEs are assigned to the reuse 3 subband. We assume that the macro network uses OFDMA and the macro UEs within each subband are assigned equal, orthogonal fractions of the subband bandwidth. In the DL, we assume each macro BS transmits equal power density to all the macro UEs. In the UL, we assume power control at each cell sets the macro UEs served in that cell to have equal receive power density. Moreover, we assume that the receive power densities are adjusted so that all cells experience an interference to thermal (IoT) of 10 dB. In both the UL and DL, the rate is then selected based on the received signal-to-interference and noise ratio (SINR). We assume that the links achieve a rate equal to 3 dB below Shannon capacity, with a maximum spectral efficiency of 5 bps/Hz.

The underlay of femtocell BSs are randomly placed with a uniform distribution at a density of 10 femto BSs per macrocell. Each femto BS serves one femto UE at a random location 20m from the femtocell BS. Note that the femtocell links are considerably smaller than the macro cell radius of 500m.

The path loss models are shown in Table II are also based on [18]. The wall loss values are the lower values in [18] under the assumption that all the macro UEs are outside,

Link	Path loss (dB)
MBS $\leftrightarrow$ MUE	$15.3 + 37.6 \log_{10}(R)$
MBS $\leftrightarrow$ FUE or FBS	$15.3 + 37.6 \log_{10}(R) + L_{ow}, L_{ow} = 10$
FBS $\leftrightarrow$ FUE (serving link)	$38.46 + 20 \log_{10}(R) + 0.7R$
FBS or FUE $\leftrightarrow$ FUE or FBS in different femtocell	$15.3 + 37.6 \log_{10}(R) + L_{ow}, L_{ow} = 20$
FBS or FUE $\leftrightarrow$ MUE	$15.3 + 37.6 \log_{10}(R) + L_{ow}, L_{ow} = 10$

TABLE II

PATH LOSS MODELS BASED ON [18].  $L_{ow}$  IS THE OUTER WALL LOSS AND  $R$  IS DISTANCE IN METERS.

each femtocell (both the BS and UE) is inside a house, with different femtocells in different houses. We have chosen the lower wall loss values, since higher values would result in a more favorable case for the proposed algorithm as the separation between the femto and macro would be greater.

Under these assumptions, we generated a random “drop” of the femto and macro network elements and then ran two simulations of the proposed femto-macro interference control algorithm in Section III: one simulation for the DL and a second for the UL. In each simulation, the load factors in the load-spillage algorithm were set in an iterative manner as follows.

In the DL, the “victims” of the femto interference are the macro UEs. Each macro UE begins by broadcasting some initial load factors across the subbands. The femto BS transmitters compute the corresponding spillage terms and then adjust their power across the subbands to maximize the rate to the femto UE. The macro UEs then compute the resulting interference and compare the interference to a target level. In this simulation, the target level was set to the interference that would degrade the rate of macro UE by no more than 10%. The load factors are then increased or decreased depending on whether the measured interference is above or below the target. The algorithm was run for 50 iterations at which point we observed that more than 99% of the macro UE experienced an interference level below 0.1 dB of the target.

Similarly, in the UL, the victims of the femto interference are the macro BS receivers. In this case, the load factors were adjusted to bound the interference rise from the femtos to 0.5 dB. This noise rise corresponds to an approximately 10% loss in rate in the power-limited regime.

The distribution of the DL and UL rates of the femto links after the final iteration of the load-spillage algorithm are shown in Fig. 3. The curves labeled “subband” are the CDFs without interference cancelation (IC), while “subband+JD” includes IC via joint detection of the macro interfering signal and desired femto signal. As a link-layer model for joint detection, we assumed the rate achievable via joint detection matched the Shannon rate with a 3dB loss in both links and maximum spectral efficiency of 5 bps/Hz.

The curves show that the load-spillage algorithm is able to deliver a large rate to a substantial fraction of the femto links. For example, in the DL, the femto links achieve a median spectral efficiency of approximately 2.6 bps/Hz without IC.

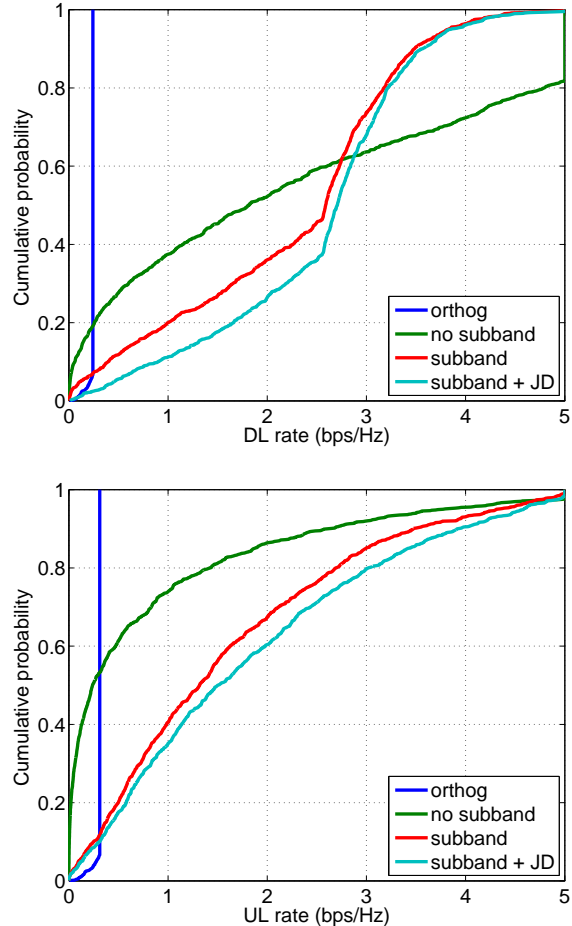


Fig. 3. Distribution of rates available on short-range links using subband scheduling with interference cancelation (“subband”), and subband scheduling with interference cancelation via joint detection of the desired femto signal and interfering macro signal (“subband+JD”). Also shown are the rate distributions with simple orthogonalization (“orthog”) and reuse 1 without subband partitioning (“no subband”). Top panel shows the DL and bottom is the UL. See text for simulation assumptions.

Moreover, the loss in macro rate due to femto interference is small. Although the target interference level was set to a maximum 10% reduction in rate in the macro, many macro UEs experience an interference well below the target. Although not shown in the figure, the actual decrease in the macro rate observed in the simulation was 4.9%.

Adding IC via joint detection can improve the rate further, especially for low rate mobiles. However, some caveats are in order: Most importantly, the gains with IC are modest. Also, our simulation assumed joint detection. In simulations of successive IC (SIC) (results are not shown), SIC alone produced only minimal gains. This is to be expected since SIC usually only has benefits for very strong interference. Since joint detection is computationally much harder than SIC, the practical value of IC may be limited.

Moving to the UL results in Fig. 3, we see that the femto links were able to achieve median spectral efficiencies of approximately 1.4 bps/Hz without IC and 1.5 bps/Hz with IC. The loss in the macro rate was somewhat higher at 6.2%,

but still small. The gains with IC in this case are minimal. This may be result of the fact that we assumed a rate fair scheduler per cell in the uplink so no macro links come at very low rate. Other macro scheduling policies may show further improvements for IC, but this needs further study.

We conclude that subband scheduling in the macro combined with the load-spillage power control in the femto can enable a large rate for many femto links with minimal effect in the macro. In addition, modest gains are possible in the DL with IC, especially at low rates.

Fig. 3 also shows a comparison of the proposed method to simple orthogonalization. In orthogonalization, the femtos and macros operate on different frequencies. Now, the proposed method resulted in a 4.9% drop in the average macro DL spectral efficiency and an 6.2% drop in the macro UL. To compare the proposed method to orthogonalization, we can subtract that fraction of the bandwidth from the macro and run the femtos with no macro interference in that bandwidth. The resulting CDF of the rates are shown in Fig. 3 on the curve labeled “orthog”. With orthogonalization from the macro, many of the femto links get the maximum rate of 5 bps/Hz times the bandwidth fraction. But, that rate is much smaller for the overwhelming majority of links.

Fig. 3 also shows the rate distribution with reuse 1 and power control without subband partitioning. This can be simulated with the above framework, but with  $K = 1$  subband. In the UL, we see that the proposed method offers significantly greater rate. In the DL, the median rate is approximately the same, although the proposed method is more fair in that the rate variation is less.

## CONCLUSIONS

We have shown that subband partitioning of the macrocell, in addition to being beneficial to the rate distribution in the macrocell network, may offer significant opportunities for simultaneous short-range communication in the same band as the macro. The key idea to realize this potential rate is for the short-range transmitters to estimate the path losses to the macro receivers and to then perform some optimal power allocation across the subbands based on the path loss estimates. In the simulation scenario considered here, the proposed method offers significantly greater rates than simple orthogonalization between the femto and macros. The proposed method also appears to outperform reuse 1 without subband partitioning in the UL. In the DL, the proposed method has a similar median rate, but shows less rate variations. Further gains are also possible with interference cancelation in the DL, but requires joint detection and not SIC alone. The gains in the UL for IC (even with joint detection) are small.

A benefit of the proposed strategy is that the short-range communication can be achieved entirely “under the radar” of the macrocell, in that there is no need for any explicit communication between the macros and short-range links. The only requirements are that the short-range transmitters must estimate the path losses to the macro receivers, the macro receivers must estimate the aggregate interference rise from the short-range links and broadcast certain load factors. The fact

that the short-range communication can share the band with minimal coordination may also be useful in other scenarios such as cognitive radios where the primary user needs operate without coordination with potential secondary users.

Further simulations are however needed. Most importantly, the current simulations have assumed perfect knowledge of the path losses and full buffer traffic without any dynamics. We have also not explicitly modeled the overhead for the signals to estimate the path losses.

## APPENDIX A PROOF OF THEOREM 1

To prove (a), fix the load factors  $s_{ik} > 0$  and power constraint bounds  $\lambda_j > 0$  and suppose that the powers  $\mathbf{p}_j$  satisfy (5). To show that the set of  $\mathbf{p}_j$ 's is Pareto optimal, suppose that there is an alternative set of power vectors  $\mathbf{p}_j^1$  with  $U(\mathbf{p}_j^1) \geq U(\mathbf{p}_j)$  for all  $j$  with strict inequality for at least one  $j$ . Let  $q_{ik}^1$  be the corresponding interference levels as in (1). We must show that  $q_{ik}^1 > q_{ik}$  for some  $i$  and  $k$ .

First observe that since  $U_j(\mathbf{p}_j)$  is strictly increasing in each  $p_{jk}$ ,  $U_j(\mathbf{p}_j^1) \geq U(\mathbf{p}_j)$  and  $\mathbf{p}_j$  is the maxima of (5) subject to (4), we must have that for all  $j$ ,

$$\sum_{k=1}^K p_{jk}^1 r_{jk} \geq \lambda_j + \epsilon_j, \quad \sum_{k=1}^K p_{jk} r_{jk} \leq \lambda_j$$

where  $\epsilon_j \geq 0$  for all  $j$  with  $\epsilon_j > 0$  for at least one  $j$ . Therefore,

$$\begin{aligned} \sum_{k=1}^K p_{jk}^1 r_{jk} &\geq \sum_{k=1}^K p_{jk} r_{jk} + \epsilon_j \\ \stackrel{(a)}{\Leftrightarrow} &\sum_{k=1}^K \sum_{i=1}^{M(k)} (p_{jk}^1 - p_{jk}) s_{ik} G_{ijk} \geq \epsilon_j \\ \stackrel{(b)}{\Rightarrow} &\sum_{j=1}^N \sum_{k=1}^K \sum_{i=1}^{M(k)} (p_{jk}^1 - p_{jk}) s_{ik} G_{ijk} > 0 \\ \stackrel{(c)}{\Rightarrow} &\sum_{k=1}^K \sum_{i=1}^{M(k)} s_{ik} (q_{ik}^1 - q_{ik}) > 0 \end{aligned}$$

where (a) follows from (3); (b) follows from taking the sum over  $j$  and using the fact that  $\epsilon_j \geq 0$  with strict inequality for at least one  $j$ ; and (c) follows from the definition of  $q_{ik}$  in (1). Since  $s_{ik} > 0$ , we must have that  $q_{ik}^1 > q_{ik}$  for at least one  $(i, k)$ . This proves part (a) of Theorem 1.

To prove the converse part (b), we need the following standard result in linear algebra.

*Lemma 1:* Suppose  $\mathbf{A} \in \mathbb{R}^{m \times n}$  is a matrix such that for any  $\mathbf{v} \in \mathbb{R}^n$ , there exists some component  $i = 1, \dots, m$  such that  $(\mathbf{A}\mathbf{v})_i \leq 0$ . Then, there exist a  $\mathbf{w} \in \mathbb{R}^m$  with  $\mathbf{w}^T \mathbf{A} = 0$ ,  $w_i \geq 0$  for all  $i$  and  $\sum_i w_i = 1$ .

*Proof:* Let  $\mathbf{W}$  be the simplex,

$$\mathbf{W} := \left\{ \mathbf{w} \in \mathbb{R}^m : w_i \geq 0, \sum_i w_i = 1 \right\}.$$

The hypothesis of the lemma implies that for every  $\mathbf{v} \in \mathbb{R}^n$ , there exists a  $\mathbf{w} \in \mathbf{W}$  such that  $\mathbf{w}^T \mathbf{A}\mathbf{v} \leq 0$ . Therefore,

$$\max_{\mathbf{v} \in \mathbb{R}^n} \min_{\mathbf{w} \in \mathbf{W}} \mathbf{w}^T \mathbf{A}\mathbf{v} = 0.$$



Since this optimization is convex in  $\mathbf{w}$  and concave in  $\mathbf{v}$ , there is a Nash equilibrium [34], so we can interchange the min and max to obtain

$$\min_{\mathbf{w} \in \mathbf{W}} \max_{\mathbf{v} \in \mathbb{R}^n} \mathbf{w}^T \mathbf{A} \mathbf{v} = 0.$$

But this can occur only if  $\mathbf{w}^T \mathbf{A} = 0$ . ■

We can use this result to prove the the converse in part (b) as follows. Suppose  $\mathbf{p}_j$ ,  $j = 1, \dots, N$  is a set of Pareto optimal powers. Since they are Pareto optimal, any small change in the powers must result in an increase in one of the interference levels  $q_{ik}$  or decrease in the utilities  $U_j$ . That is, for any non-zero set of  $\Delta p_{jk}$ 's, there must either be some  $i$  and  $k$  such that

$$\Delta q_{ik} := \sum_j G_{ijk} \Delta p_{jk} \geq 0, \quad (6)$$

or  $j$  such that

$$\Delta U_j := \frac{\partial U_j(\mathbf{p}_j)}{\partial p_{jk}} \Delta p_{jk} \leq 0. \quad (7)$$

Define the matrix  $\mathbf{A}$  by

$$\mathbf{A} = \begin{bmatrix} -DU(\mathbf{p}) \\ \mathbf{G} \end{bmatrix},$$

where the columns are indexed by the pairs  $(j, k)$ ,  $DU(\mathbf{p})$  is the matrix with the components  $DU(\mathbf{p})_{j,jk} = \partial U_j(\mathbf{p}_j) / \partial p_{jk}$  and  $\mathbf{G}$  is the matrix of gains  $G_{i,jk}$ . Now, (6) and (7) shows that for every  $\Delta \mathbf{p}$ ,  $(\mathbf{A} \Delta \mathbf{p})_\ell \leq 0$  for some index  $\ell$ . Hence, by Lemma 1, there must exist a  $\mathbf{w} \geq 0$  with unit norm such that  $\mathbf{w}^T \mathbf{A} = 0$ . Partitioning

$$\mathbf{w} = [\mathbf{t}^T \ \mathbf{s}^T]^T$$

conformably with  $\mathbf{A}$  we see that there exists a set of nonnegative  $t_j$  and  $s_{ik}$  such that

$$t_j \frac{\partial U_j(\mathbf{p}_j)}{\partial p_{jk}} - \sum_{i=1}^{M(k)} s_{ik} G_{ijk} = 0. \quad (8)$$

Now  $t_j \geq 0$  for all  $j$  and  $s_{ik} \geq 0$  for all  $i$  and  $k$ , with at least one of the parameters being strictly greater than zero. Since  $G_{ijk} > 0$  and  $\partial U_j / \partial p_{jk} > 0$  for all  $i, j$  and  $k$ , it can be verified that (8) implies that  $t_j > 0$  for all  $j$ .

Now, using (3), (8) can be rewritten as

$$\frac{\partial L_j(\mathbf{p}_j)}{\partial p_{jk}} = 0, \quad (9)$$

where  $L_j$  is the Lagrangian

$$L_j(\mathbf{p}_j) := t_j U_j(\mathbf{p}_j) - \sum_{k=1}^K r_{jk} p_{jk}.$$

Let  $\lambda_j = \sum_k r_{jk} p_{jk}$ . Since  $t_j > 0$ , (9) shows that  $\mathbf{p}_j$  is a critical point of the optimization (5) subject to (4). Since  $U_j(\mathbf{p}_j)$  is concave, any critical point is the maxima. Thus, we have found  $s_{ik}$  and  $\lambda_j$  such that the set of power vectors  $\mathbf{p}_j$  satisfy (5).

## REFERENCES

- [1] 3GPP, "UTRAN architecture for 3G Home Node B (HNB); Stage 2," TS 25.467 (release 9), 2010.
- [2] —, "Service requirements for Home NodeBs (UMTS) and eNodeBs (LTE)," TS 22.220 (release 9), 2010.
- [3] —, "3G Home NodeB Study Item Technical Report," TR 25.820 (release 9), 2010.
- [4] V. Chandrasekhar, J. G. Andrews, and A. Gatherer, "Femtocell networks: A survey," *IEEE Comm. Mag.*, vol. 46, no. 9, pp. 59–67, Sep. 2009.
- [5] S.-P. Yeh, S. Talwar, S.-C. Lee, and H. Kim, "WiMAX femtocells: A perspective on network architecture, capacity, and coverage," *IEEE Comm. Mag.*, vol. 46, no. 10, pp. 58–65, Oct. 2008.
- [6] D. López-Pérez, A. Valcarce, G. de la Roche, and J. Zhang, "OFDMA femtocells: A roadmap on interference avoidance," *IEEE Comm. Mag.*, vol. 47, no. 9, pp. 41–48, Sep. 2009.
- [7] H. Claussen, "Co-channel operation of macro- and femtocells in a hierarchical cell structure," *Int. J. Wireless Information Networks*, vol. 15, no. 3–4, pp. 137–147, Dec. 2008.
- [8] Huawei, "Soft Frequency Reuse Scheme for UTRAN LTE," 3GPP R1-050507, May 2005.
- [9] H. Lei, L. Zhang, X. Zhang, and D. Yang, "A novel multi-cell OFDMA system structure using fractional frequency reuse," in *Proc. Personal Indoor Mobile Radio Comm.*, Athens, Greece, Sep. 2007.
- [10] S. Han, J. Park, T.-J. Lee, H.G.Ahn, and K. Jang, "A new frequency partitioning and allocation of subcarriers for fractional frequency reuse in mobile communication systems," *IEICE Trans. Comm.*, no. 8, p. 27482751.
- [11] A. Stolyar and H. Viswanathan, "Self-organizing dynamic fractional frequency reuse in OFDMA systems," in *Proc. IEEE INFOCOM*, Phoenix, AZ, Apr. 2009, pp. 691–698.
- [12] C. Y. Oh, M. Y. Chung, H. Choo, and T.-J. Lee, "A Novel Frequency Planning for Femtocells in OFDMA-Based Cellular Networks Using Fractional Frequency Reuse," in *Computational Science and Its Applications ICCSA 2010*, Fukuoka, Japan, Mar. 2010, pp. 96–106.
- [13] P. Hande, S. Rangan, M. Chiang, and X. Wu, "Distributed uplink power control for optimal SIR assignment in cellular data networks," *IEEE/ACM Trans. Networking*, vol. 16, no. 6, pp. 1420–1433, Dec. 2008.
- [14] J. Zhang and G. de la Roche, *Femtocells: Technologies and Deployment*. John Wiley & Sons, 2010.
- [15] Z. Shi and M. C. Reed, "Iterative maximal ratio combining channel estimation for multiuser detection on a time frequency selective wireless CDMA channel," in *Proc. IEEE Wireless Communications and Networking Conference*, Hong Kong, Mar. 2007.
- [16] V. Chandrasekhar, J. G. Andrews, T. Muharemovic, Z. Shen, and A. Gatherer, "Power control in two-tier femtocell networks," *IEEE Trans. Wireless Comm.*, vol. 8, no. 8, pp. 4316–4328, Aug. 2009.
- [17] H.-S. Jo, C. Mun, J. Moon, and J.-G. Yook, "Interference mitigation using uplink power control for two-tier femtocell networks," *IEEE Trans. Wireless Comm.*, vol. 8, no. 10, pp. 4906–4910, Oct. 2009.
- [18] FemtoForum, "Interference Management in OFDMA Femtocells," Whitepaper available at [www.femtoforum.org](http://www.femtoforum.org), Mar. 2010.
- [19] S. Kishore, L. J. Greenstein, H. V. Poor, and S. C. Schwartz, "Capacity in a CDMA Macrocell with a Hotspot Microcell: Exact and Approximate Analyses," in *Proc. IEEE Veh. Tech. Conf.*, Atlantic City, NJ, Oct. 2001, pp. 1172–1176.
- [20] —, "Soft handoff and uplink capacity in a two-tier CDMA system," *IEEE Trans. Wireless Comm.*, vol. 4, no. 4, pp. 1297–1301, Jul. 2005.
- [21] V. Chandrasekhar and J. G. Andrews, "Uplink capacity and interference avoidance for two-tier femtocell networks," *IEEE Trans. Wireless Comm.*, vol. 8, no. 7, pp. 3498–3509, July 2009.
- [22] —, "Spectrum allocation in tiered cellular networks," *IEEE Trans. Comm.*, vol. 57, no. 10, pp. 3059–3068, Oct. 2009.
- [23] E. Dahlman, S. Parkvall, J. Sköld, and P. Beming, *3G Evolution: HSPA and LTE for Mobile Broadband*. Oxford, UK: Academic Press, 2007.
- [24] R. Ahlswede, "Multi-way communication channels," in *Proc. IEEE Int. Symp. Inform. Th., Armenian S.S.R.*, Sep. 1971, pp. 23–52.
- [25] T. M. Cover and J. A. Thomas, *Elements of Information Theory*. New York: John Wiley & Sons, 1991.
- [26] J. G. Andrews, "Interference cancellation for cellular systems: A contemporary overview," *IEEE Wireless Comm.*, vol. 12, no. 2, pp. 19–29, Apr. 2005.
- [27] G. Boudreau, J. Panicker, N. Guo, R. Chang, N. Wang, and S. Vrzic, "Interference Coordination and Cancellation for 4G Networks," *IEEE Comm. Mag.*, vol. 47, no. 4, pp. 74–81, Apr. 2009.



- [28] K. Yeung and S. Nanda, "Channel management in microcell/macrocell cellular radio systems," *IEEE Trans. Vehicular Tech.*, vol. 45, no. 4, pp. 601–612, Nov. 1996.
- [29] B. Jabbari and W. F. Fuhrmann, "Teletraffic modeling and analysis of flexible hierarchical cellular networks with speed-sensitive handoff strategy," *IEEE J. Sel. Areas Comm.*, vol. 15, no. 8, pp. 1539 – 1548, Oct. 1997.
- [30] T. E. Klein and S.-J. Han, "Assignment strategies for mobile data users in hierarchical overlay networks: performance of optimal and adaptive strategies," *IEEE J. Sel. Areas Comm.*, vol. 22, no. 5, pp. 849–861, Jun. 2004.
- [31] M. Chiang, P. Hande, T. Lan, and C. W. Tan, "Power Control in Wireless Cellular Networks," *Foundation and Trends in Networking*, vol. 2, no. 4, pp. 381–533, Jul. 2008.
- [32] W. Yu, G. Ginis, and J. Cioffi, "Distributed multiuser power control for digital subscriber lines," *IEEE J. Sel. Areas Comm.*, vol. 20, no. 5, p. 11051115, Jun. 2002.
- [33] R. Cendrillon, J. Huang, M. Chiang, and M. Moonen, "Autonomous Spectrum Balancing for Digital Subscriber Lines," *IEEE Trans. Signal Process.*, vol. 55, no. 8, pp. 4241–4257, Aug. 2007.
- [34] S. P. Boyd, L. El Ghaoui, E. Feron, and V. Balakrishnan, *Linear Matrix Inequalities in System and Control Theory*. Philadelphia, PA: SIAM, 1994.